Conclusion

Using the difference in energy distribution for circular waves transmitted through ferrite loaded circular waveguide, an isolator was constructed with 30 db isolation from 8 to 11 kmc. Its insertion loss is less than 3 db and it does not appear to be unduly critical with respect to any of the operating parameters. By providing means for varying the applied field the isolator becomes an amplitude modulator or electronic switch.

Since the energy transmitted in the forward direction tends to go around the ferrite, low magnetic and dielectric losses occur in it. This approach to isolation is promising for higher powers. A more suitable choice of material will reduce the insertion loss presently observed.

The frequency of maximum isolation for a single ferrite rod is inversely proportional to the ferrite diameter. Various diameter rods can be added in series to increase the isolation bandwidth. However, with the ferrite used an increase in insertion loss on the high frequency side discourages this beyond a 3 kmc bandwidth. The increase in insertion loss which occurs at higher frequencies is attributable to dielectric waveguide effects for the positive wave. With a dielectric constant of 13 the $\mu\epsilon$ product is large even if μ is as low as 0.3. In such a case, dielectric waveguide type transmission is expected to become noticeable at 11 kmc.

The use of differential energy distribution for nonreciprocal and magnetically controllable circuit elements is promising from the standpoint of stability, bandwidth, and power handling capacity.

Acknowledgment

The authors wish to thank Dr. A. L. Aden for his assistance in planning the project which led to this work, and for his helpful suggestions during the course of the work. We also wish to thank Mr. M. Medina for making many of the microwave measurements.

An Approximate Analysis of Coaxial Line with a Helical Dielectric Support*

J. W. E. GRIEMSMANN†

SHOWN in Fig. 1 is a cutaway section of coaxial cable with a helical dielectric support. The particular cable depicted bears the trade name of Styroflex[1] derived from the fact that the dielectric helix is built up in a winding operation from nonplasticized polystyrene tapes giving to the final assembly a tight grip on the center conductor and a good degree of allowable bending capability. The outer conductor in the original design of the cable consists of an aluminum sheath extruded over the dielectric. Other forms of cable with helical dielectric support are also available.

This type of cable is of interest as an alternative to broadband bead supported line, particularly for applications requiring long lengths of line or small diameter cable where multiplicity of bead supports can lead to high wave reflection characteristics in frequency bands of interest.

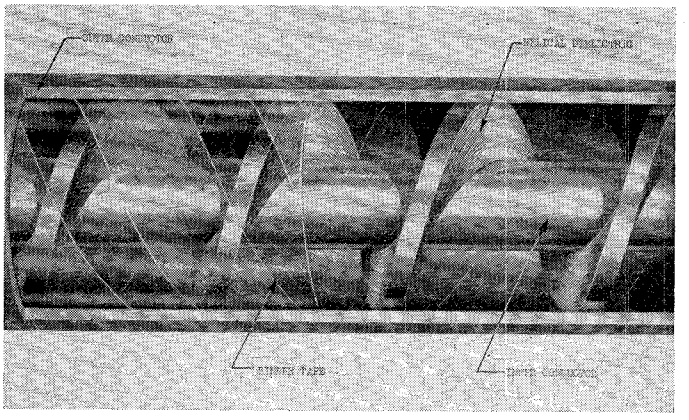

Fig. 1—Cut-away section of Styroflex cable.

The analysis given below shows that the total propagation in the helical line can be considered to be made up of two component propagations, one following the dielectric helix down the transmission line and the other following a helical path perpendicular to the dielectric. The latter type of propagation is that of an iterative transmission line and introduces for the overall propa-

* This analysis was conducted as part of the work under Signal Corps Contract DA-36-039 sc-42500 with the Polytechnic Institute of Brooklyn and was presented at the P.I.B. Symposium on Modern Advances in Microwave Techniques, November 8–10, 1954.

† Microwave Res. Inst., Polytechnic Inst. of Brooklyn, Bklyn., N. Y.

[1] Phelps Dodge Copper Products Corp.

gation characteristics of the line bands of propagation and attenuation. For practical purposes, operation is limited to frequencies approaching the first critical frequency which occurs approximately when the helical distance at the mean internal periphery measures an electrical half-wavelength between centers of the dielectric. The low frequency approximation which neglects the helical distribution of the dielectric and assumes the air and dielectric of the line to act in parallel is a satisfactory one for a major portion of the lowest propagating frequency region. The analysis given here shows a sharp rise in attenuation as the cutoff frequency is approached. This action is quantitatively confirmed by attenuation measurements on the transmission line.

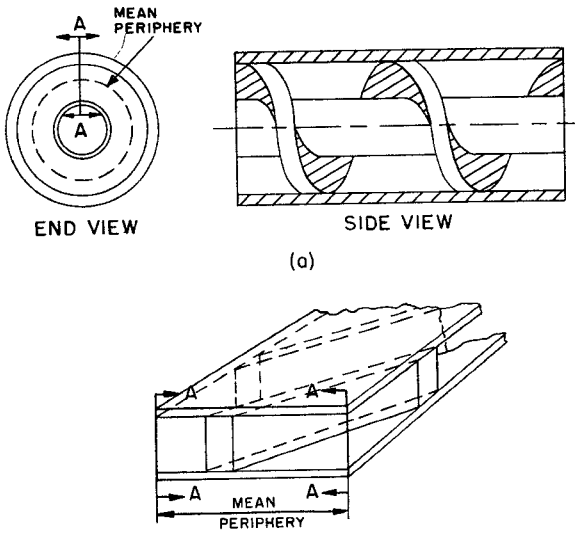

Fig. 2

Parallel Plate Approximation

The following analysis is based on the transformation of the problem in coaxial geometry to one in parallel plate geometry. Consider that the coaxial line shown in Fig. 2(a) is split radially from the outer conductor into the inner conductor along the line AA and for the entire length of coaxial line. Opening the line along this cut and continuously deforming it the parallel plate structure of Fig. 2(b) can be attained where the radial cut plane of the coaxial line splits into the two side planes through AA for the parallel plate line. It must now be understood, of course, that a condition for the parallel plate propagation is that the fields are identical in the side planes in order that the parallel plate line can again be reformed back into the original coaxial line. The parallel plate structure of Fig. 2(b) is considered to be part of a larger parallel plate system, the top view of which is shown in Fig. 3, since it would be inappropriate to consider edge effects for the parallel plate. The region of interest from the propagation standpoint is that between the two side planes through A-A. The mode and nature of propagation in the parallel plate line will now be very similar to that in the original coaxial line although any numerical values obtained represent an approximation to the values existing in the coaxial line. The rigorous solution in suitable radial or helical coordinates is required for exact values for the propagation characteristics and fields of lines with helical supports.

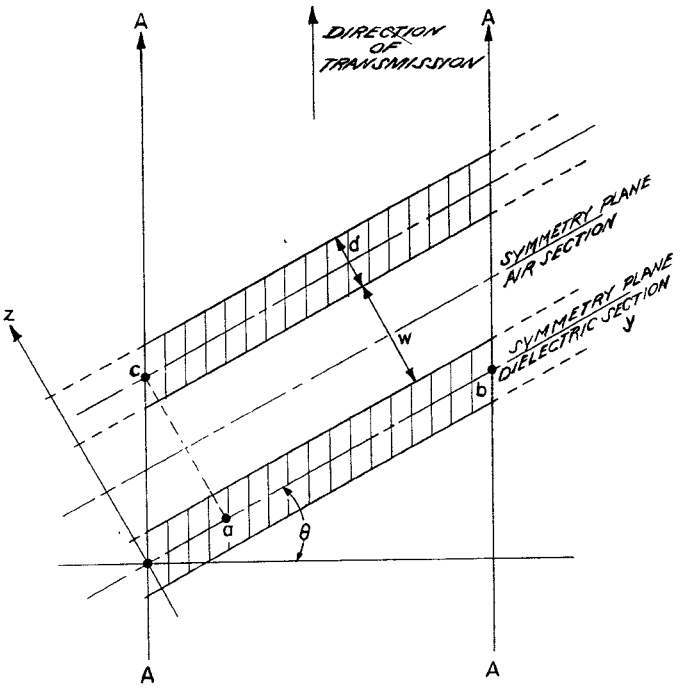

Fig. 3—Top view of extended parallel plate system.

Field Components

In any fundamental mode type of propagation in the parallel plate system there must be assumed to exist an electrical field perpendicular to the plates. This corresponds to a radial electric field in the coaxial line. The existence of this electric field component E_x which is noted to be directed parallel to the dielectric surface would require in general the two components H_y and H_z to exist in order to satisfy the boundary conditions corresponding to refraction at the air-dielectric interface. By trial the simplest mode which would satisfy the Maxwell's equations and boundary conditions was found to be the following set:

In Air Sections

$$H_{yo} = \frac{k_{zo}}{\omega\mu} A_o[1 - \Gamma_o\epsilon^{+2jk_{zo}z'}]\epsilon^{-jk_{zo}z'}\epsilon^{-jk_y y} \tag{1}$$

$$H_{zo} = -\frac{k_y}{\omega\mu} A_o[1 + \Gamma_o\epsilon^{+2jk_{zo}z'}]\epsilon^{-jk_{zo}z'}\epsilon^{-jk_y y} \tag{2}$$

$$E_{xo} = A_o[1 + \Gamma_o\epsilon^{+2jk_{zo}z'}]\epsilon^{-jk_{zo}z'}\epsilon^{-jk_y y} \tag{3}$$

where z' is measured from the symmetry planes of the air sections.

In Dielectric Sections

$$H_{y\epsilon} = \frac{k_{z\epsilon}}{\omega\mu} A_\epsilon [1 - \Gamma_\epsilon \epsilon^{+2jk_{z\epsilon}z''}] \epsilon^{-jk_{z\epsilon}z''} \epsilon^{-jk_y y} \quad (4)$$

$$H_{z\epsilon} = -\frac{k_y}{\omega\mu} A_\epsilon [1 + \Gamma_\epsilon \epsilon^{+2jk_{z\epsilon}z''}] \epsilon^{-jk_{z\epsilon}z''} \epsilon^{-jk_y y} \quad (5)$$

$$E_{x\epsilon} = A_\epsilon [1 + \Gamma_\epsilon \epsilon^{+2jk_{z\epsilon}z''}] \epsilon^{-jk_{z\epsilon}z''} \epsilon^{-jk_y y} \quad (6)$$

where z'' is measured from the symmetry planes of the dielectric sections.

With low losses a suitable approximation is that k_{zo}, $k_{z\epsilon}$ and k_y are respectively the phase constants in the z direction in air, in the z direction in the dielectric and in the y direction. The same phase constant k_y in the air and dielectric is necessary to satisfy the boundary condition along the air-dielectric interface. A_o and A_ϵ are complex constants indicating the relative magnitudes and phase of the field. The field distribution in the cross section is determined by the reflection coefficient Γ_o in the air sections and Γ_ϵ that in the dielectric sections. It is implicitly assumed that the field is periodic in the z direction and that the values of the complex constants A_o, A_ϵ, Γ_o and Γ_ϵ are determined by boundary conditions at the air-dielectric interface, transmission conditions and the power being transmitted.

For convenience in the understanding of the propagation characteristics of the line, it is desirable to consider that the total propagation is made up of two partial propagations in parallel, one in the y direction associated with the components E_x and H_z, and the other in the z direction associated with E_x and H_y. The propagation in the y direction or in the direction parallel to the dielectric has associated with it a constant cross section and only one forward traveling wave is needed to describe this propagation. The propagation in the z direction must be considered as an iterative transmission line having successive sections of air and dielectric. In order to satisfy the boundary conditions (or impedance conditions) at the air-dielectric boundaries, it is necessary to postulate forward and backward traveling waves (or to include the reflection coefficients) in each medium just as one would for an ordinary iterative transmission line structure. As seen later, reflection coefficients are real at lines of symmetry in the air and dielectric sections making them convenient reference points for extensions Z' and Z'' in z direction.

Phase Constant Relationships

The propagation constants in the y direction and z direction must be consistent with the over-all propagation constant in each of the media. Thus, in the dielectric sections,

$$k_{z\epsilon}^2 + k_y^2 = k_\epsilon k^2 \quad (7)$$

where k is free space phase constant and k_ϵ is relative dielectric constant of medium. In air section

$$k_{zo}^2 + k_y^2 = k^2 \quad (8)$$

where k for the air is assumed equal to that of free space.

In order to satisfy the condition that for the section of the parallel plate line the fields in the side planes must be identical, it is required that the phase of the field at the points, b and c, shown in Fig. 3 must be identical. This gives rise to another condition on the phase constants which may be derived by requiring that the change in phase of field experienced in going from the point a to b in Fig. 3 is the same as the change in phase in going from the point a to the point c. The resulting equation for this condition must be derived from iterative line considerations.

Propagation Characteristics in the z Direction

In the z direction, the transmission line structure is periodic and symmetrical with respect to propagation in the forward or backward z direction. The description for arbitrary terminating impedance is then conveniently given in terms of iterative impedances. Shown in Fig. 4(a) is the equivalent transmission line (for wave impedances) in the z direction for the extended parallel plate structure. Also shown in this figure, plotted on an admittance diagram, is a typical admittance cycle representing the locus of impedances of the transmission line matched in its iterative impedance. In general, of course, for this type of operation there will be standing waves in both the air sections and dielectric sections of the line but the iterative impedance matching implies that the magnitude of electric and magnetic field is repeated at successive corresponding structural points along the transmission line. Since for any transverse plane the points at the special AA side planes, described before in Fig. 3, are corresponding structural points in the iterative transmission, the boundary condition that the fields be identical at corresponding transverse side plane points is in part satisfied. The requirement of the boundary condition then remaining is that the phase be identical at the corresponding transverse side points. Determination of the phase constant for the iterative type transmission line in the y direction is then required. This solution will also yield the values of Γ_o and Γ_ϵ necessary for a quantitative knowledge of the field structure and the determination of attenuation constant for this line.

For further analytical work, one of the two most convenient sets of reference planes in the iterative structure is the centers of the air sections corresponding to the real admittance points Y_{co} on the admittance cycle. Shown in Fig. 4(b) is the structure between two successive reference planes terminated in the iterative impedances Y_{co}. Since the section is symmetrical, the value Y_{co} can be determined from

$$Y_{oc} = \sqrt{Y_{op(1/2)}\ Y_{sh(1/2)}} \quad (9)$$

where $Y_{op(1/2)}$ is the admittance measured at the input, a, with an open circuit at the center reference plane, d, and $Y_{sh(1/2)}$ is the admittance measured at the input with a short circuit at the center reference plane d.

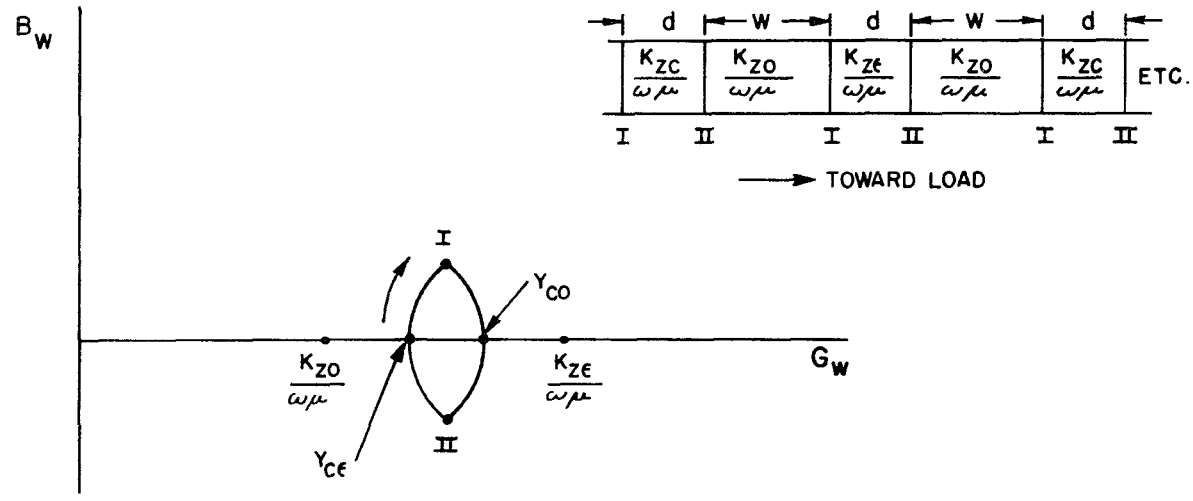

(a) SCHEMATIC ADMITTANCE CYCLE DIAGRAM

ITERATIVE TRANSMISSION LINE
(Z - DIRECTION)

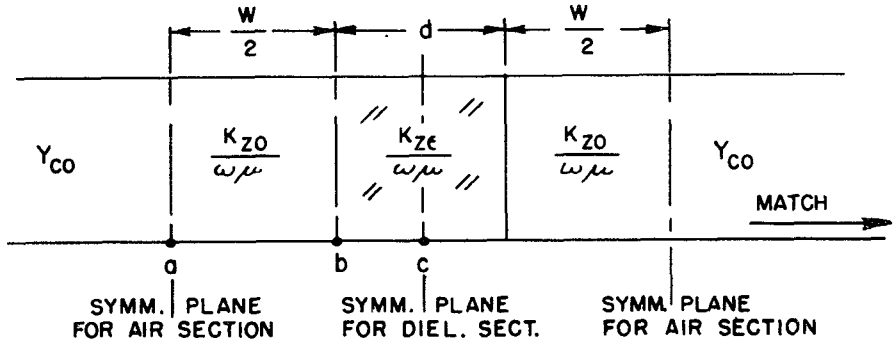

(b) COMPOSITE SYMMETRICAL SECTION

Fig. 4.

From transmission line calculations, the values of these admittances are determined to be the following:

$$Y_{op(1/2)} = j\frac{k_{zo}}{\omega\mu}\tan\left[k_{zo}\frac{w}{2} + \tan^{-1}\left(\frac{k_{z\epsilon}}{k_{zo}}\tan k_{z\epsilon}\frac{d}{2}\right)\right] \quad (10)$$

$$Y_{sh(1/2)} = -j\frac{k_{zo}}{\omega\mu}\cot\left[k_{zo}\frac{w}{2} + \tan^{-1}\left(\frac{k_{zo}}{k_{z\epsilon}}\tan k_{z\epsilon}\frac{d}{2}\right)\right] \quad (11)$$

whence

$$Y_{co}^2 = \left(\frac{k_{zo}}{\omega\mu}\right)^2 \frac{\tan\left[k_{zo}\frac{w}{2} + \tan^{-1}\left(\frac{k_{z\epsilon}}{k_{zo}}\tan k_{z\epsilon}\frac{d}{2}\right)\right]}{\tan\left[k_{zo}\frac{w}{2} + \tan^{-1}\left(\frac{k_{zo}}{k_{z\epsilon}}\tan k_{z\epsilon}\frac{d}{2}\right)\right]}; \quad (12)$$

the value of the reflection coefficient Γ_o at the center plane of the air section is then

$$\Gamma_o = \frac{1 - \left(\frac{\omega\mu Y_{co}}{k_{zo}}\right)}{1 + \left(\frac{\omega\mu Y_{co}}{k_{zo}}\right)}. \quad (13)$$

Alternatively, the reference planes for the start and finish of the composite line could have been selected as the center or symmetry planes for the dielectric sections which would correspond to the admittance $Y_{c\epsilon}$ on the schematic admittance cycle diagram of Fig. 4. By appropriate substitution of variables the value of the characteristic admittance would be found to be given by

$$Y_{c\epsilon}^2 = \left(\frac{k_{z\epsilon}}{\omega\mu}\right)^2 \frac{\tan\left[k_{z\epsilon}\frac{d}{2} + \tan^{-1}\left(\frac{k_{zo}}{k_{z\epsilon}}\tan k_{zo}\frac{w}{2}\right)\right]}{\tan\left[k_{z\epsilon}\frac{d}{2} + \tan^{-1}\left(\frac{k_{z\epsilon}}{k_{zo}}\tan k_{zo}\frac{w}{2}\right)\right]} \quad (14)$$

giving for

$$\Gamma_\epsilon = \frac{1 - \left(\frac{\omega\mu Y_{c\epsilon}}{k_{z\epsilon}}\right)}{1 + \left(\frac{\omega\mu Y_{c\epsilon}}{k_{z\epsilon}}\right)}. \quad (15)$$

For the structure shown in Fig. 4(b) the change in phase from input to output, Φ_I, is determined from iterative line considerations, being given by

$$\cos \Phi_I = \cos k_{z\epsilon} d \cos k_{zo} w - \frac{1}{2}\left(\frac{k_{z\epsilon}}{k_{zo}} + \frac{k_{zo}}{k_{z\epsilon}}\right) \sin k_{z\epsilon} d \sin k_{zo} w. \quad (16)$$

In order to satisfy the boundary condition, corresponding transverse points at the side planes must have the same phase as previously discussed under PHASE CONSTANT RELATIONSHIPS. Then, with reference to points b and c of Fig. 3, it is evident that

$$\Phi_I = k_y \frac{w + d}{\tan \theta} \pm n(2\pi) \quad (17)$$

whence

$$\cos k_y \frac{w + d}{\tan \theta} = \cos k_{z\epsilon} d \cos k_{zo} w - \frac{1}{2}\left(\frac{k_{z\epsilon}}{k_{zo}} + \frac{k_{zo}}{k_{z\epsilon}}\right) \sin k_{z\epsilon} d \sin k_{zo} w. \quad (16a)$$

The phase constants k_y, $k_{z\epsilon}$ and k_{zo} are now specified in terms of the dimensions, w, d, and θ, and the frequency or free space phase constant, k, through (7), (8), and (16a). The form of the field can then be specified at any frequency from an evaluation of Γ_o and Γ_ϵ, using (12) through (15). In the expression relating Φ_I and k_y above $n = 0$ corresponds to the lowest practical range of operation with a cutoff frequency of zero. Integer values of n correspond to higher mode operation having finite cutoff frequencies. The wavelength in the transmission direction (λ_g) may be determined from

$$k_g = \frac{2\pi}{\lambda_g} = \frac{k_y}{\sin \theta}. \quad (18)$$

LOW FREQUENCY APPROXIMATION

The low frequency approximation can be deduced directly from the consideration that dielectric and air sections act in parallel. The solution above reduces to this solution under the assumption of sufficiently low frequencies. For low frequencies, (16a) becomes under the assumption that typically $\sin \alpha = \alpha$ and $\cos \alpha = 1 - (\alpha^2/2)$

$$\left(k_y \frac{w + d}{\tan \theta}\right)^2 = (k_{z\epsilon}^2 d + k_{zo}^2 w)(w + d). \quad (16b)$$

Using (7) and (8), the phase constants become

$$k_y = k\left(\frac{k_\epsilon d + w}{w + d}\right)^{1/2} \sin \theta = k\, k_{eff}^{1/2} \sin \theta \quad (16c)$$

$$k_{z\epsilon} = k(k_\epsilon - k_{eff} \sin^2 \theta)^{1/2} \quad (7a)$$

$$k_{zo} = k(1 - k_{eff} \sin^2 \theta)^{1/2}. \quad (8a)$$

As indicated the expression

$$\left(\frac{k_\epsilon d + w}{w + d}\right)$$

is recognized to be the effective relative dielectric constant under the assumption that the dielectric sections and air sections are acting in parallel. For the iterative line in the z direction, the admittance cycle diagram of Fig. 4(a) reduces at low frequencies to a point for the values of iterative wave admittances from (12) and (14)

$$Y_{io} = Y_{c\epsilon} = \frac{k}{\omega\mu}\left[\frac{k_{z\epsilon}^2 d + k_{zo}^2 w}{k^2(w + d)}\right]^{1/2} = \frac{k}{\omega\mu} k_{eff}^{1/2} \cos \theta.$$

The expressions for the fields in the air sections become from (1), (2), and (3),

$$E_{xo} = A_o \frac{2(1 - k_{eff} \sin^2 \theta)^{1/2}}{(1 - k_{eff} \sin^2 \theta)^{1/2} + k_{eff}^{1/2} \cos \theta} \quad (3a)$$

$$H_{yo} = \frac{k}{\omega\mu} E_{xo} k_{eff}^{1/2} \cos \theta \quad (1a)$$

$$H_{zo} = \frac{k}{\omega\mu} E_{xo} k_{eff}^{1/2} \sin \theta. \quad (2a)$$

For fields in dielectric sections from (4), (5), and (6)

$$E_{x\epsilon} = A_\epsilon \frac{2(k_\epsilon - k_{eff} \sin^2 \theta)^{1/2}}{(k_\epsilon - k_{eff} \sin^2 \theta) + k_{eff}^{1/2} \cos \theta} \quad (6a)$$

$$H_{y\epsilon} = \frac{k}{\omega\mu} E_{x\epsilon} k_{eff}^{1/2} \cos \theta \quad (4a)$$

$$H_{z\epsilon} = \frac{k}{\omega\mu} E_{x\epsilon} k_{eff}^{1/2} \sin \theta. \quad (5a)$$

The total magnetic field in both the air and dielectric sections is noted to be transverse to the direction of propagation and to have the value

$$H_T = E_{xo} \frac{k}{\omega\mu} k_{eff}^{1/2} = E_{x\epsilon} \frac{k}{\omega\mu} k_{eff}^{1/2}.$$

The wave impedance is noted to be the same for both the air and dielectric sections supporting the low frequency assumption of TEM propagation in a homogeneous dielectric material, having a dielectric constant equal to the effective value given above. The propagation constant is that for a material with the effective dielectric constant, k_{eff}.

MODES OF OPERATION

In general, the field pattern and the consequent performance characteristics of this type of transmission line are dependent on two factors. The first of these is, of course, the requirement that the phase is identical at corresponding transverse side points as indicated in Fig. 3 and covered by (16) and (17). The second factor is the type of propagation in the z direction which, because of its iterative nature, will have pass and stop bands as indicated by either (12) or (14). The influence of the second factor is dependent on the construction of the cable, being greater for smaller pitch angle, θ, and greater influence of the dielectric. As the pitch angle approaches $\pi/2$, the line is seen to approach a line with a longitudinal dielectric support. In this case the propagation in the z direction is not a significant part of the

over-all propagation, but serves rather to determine the cutoff frequencies of the higher modes and the variation with frequency of the guide wavelengths for these higher modes.

While the foregoing analysis is applicable for any type of cable construction, consideration here will be limited to the case where the component propagation in the z direction is a significant part of the total propagation. Of chief concern will be the possible frequency limitations on the lowest mode of operation. The higher modes associated with a periodic variation of field with the coordinate x (perpendicular to plates) are not considered since, for the usual coaxial lines dimensions, the variation with y and z (parallel to plate) will impose greater limitations.

The critical frequencies for propagation in the z direction are those for which the iterative admittances, as given by (12) and (14), become infinite or zero and are the boundaries between purely propagating and purely attenuating bands. Shown in Table I are the

TABLE I
CRITICAL FREQUENCY RELATIONSHIPS

Desig	Determinental Equation	Value of[2] $\cos \Phi_I$	z Direction Wave Impedance	
			At center of Air Sections	At center of Dielectric Sections
A	$k_{z\epsilon} \tan \frac{k_{z\epsilon} d}{2} - k_{zo} \cot \frac{k_{zo} w}{2}$	-1	Short	Open
B	$k_{z\epsilon} \cot \frac{k_{z\epsilon} d}{2} = k_{zo} \tan \frac{k_{zo} w}{2}$	-1	Open	Short
C	$k_{z\epsilon} \tan \frac{k_{z\epsilon} d}{2} = -k_{zo} \tan \frac{k_{zo} w}{2}$	$+1$	Open	Open
D	$k_{z\epsilon} \cot \frac{k_{z\epsilon} d}{2} = -k_{zo} \cot \frac{k_{zo} w}{2}$	$+1$	Short	Short

[2] See (16).

formulas which define these critical frequencies listed in order of increasing frequency for a given value of n in (17). These values could also have been obtained by letting $\cos \Phi_I = \pm 1$ in (16), as indicated in Table I, or that Φ_I is an appropriate multiple of π. For any given critical frequency condition of Table I and any given value n, the critical frequency is determined using (17), (7), and (8). Operation down to zero frequency can occur only for the case $n = 0$. In this case, the infinite sequence of alternating pass and stop bands, defined by the conditions A, B, C, and D, have a propagating region between zero frequency and that of condition A. For other values of n, there will be non-zero cutoff frequencies and the sequence of pass and stop bands can be of opposite character to that for $n = 0$. The value of $k_y(w+d)/\tan \theta$ assumes values equal to multiples of π and the value zero for critical frequencies of A, B, C, and D. The value of k_y will, however, vary with frequency making the main direction of propagation a function of frequency. Total propagation in the z direction, for example, is obtained only at cutoff frequencies for which k_y can be zero, as can be noted from (2) and (5). Increasing frequency above these cutoff values will cause propagation to start in the y direction. The modes of operation then can only be characterized by n which can assume positive or negative values. Since there is a wide variation of the positioning of critical frequencies with respect to cable construction, it appears best to reserve further discussion of the modes of operation to specific cable constructions.

POWER FLOW

From (1), (2), and (3), the Poynting vector for the air sections of the line is found to be

$$\begin{aligned} |P_o &= R_e\{|E \times |H^*\} \\ &= R_e\{x_o E_x \times [y_o H_y + z_o H_z]\} \\ &= \frac{|A_o|^2}{\omega\mu}[z_o k_{zo}(1 - |\Gamma_o|^2) \\ &\quad + y_o k_y |1 + \Gamma_o \epsilon^{j k_{zo} z'}|^2] \end{aligned} \tag{19}$$

where x_o, y_o, and z_o are respectively the unit vectors in the x, y, and z directions. The power in the z direction is noted to be independent of position in the line, but to be a function of frequency through the dependence of $|\Gamma_o|^2$ on frequency. When the line is propagating in its lowest mode Γ_o is a minimum, $\Gamma_o = -|\Gamma_o|$, at the center reference plane making the y component of Poynting vector a minimum at the center of the air section.

From (4), (5), and (6), the Poynting vector for the dielectric section of the line is found to be

$$\begin{aligned} |P_\epsilon &= \frac{|A_\epsilon|^2}{\omega\mu}[z_o k_{z\epsilon}(1 - |\Gamma_\epsilon|^2) \\ &\quad + y_o k_y |1 + \Gamma_\epsilon \epsilon^{+j 2 k_{z\epsilon} z''}|^2]. \end{aligned} \tag{20}$$

The total power flow crossing a given cross section of the transmission line may be obtained by appropriately summing the amounts of power flowing in the two directions and for both air and dielectric, as shown schematically in Fig. 5.

The power in the air section in the z direction crossing any given transverse cross section is

$$P_{zo} = \frac{k_{zo}}{\omega\mu} |A_o|^2 [1 - |\Gamma_o|^2] \frac{wh}{\tan \theta}$$

where h is the height of the line and using the projected area of the air portion of cross sectional area on a z = constant plane as shown in Fig. 5.

The power in the dielectric section in the z direction crossing any given transverse cross section is

$$P_{z\epsilon} = \frac{k_{z\epsilon}}{\omega\mu} |A_\epsilon|^2[1 - |\Gamma_\epsilon|^2] \frac{dh}{\tan\theta}.$$

The power in the air section in the y direction crossing any given cross section is

$$P_{yo} = \frac{k_y}{\omega\mu} |A_o|^2 h \int_{-w/2}^{+w/2} (1 + |\Gamma_o|^2 - 2|\Gamma_o| \cos 2k_{zo}z')\, dz'$$

where propagation conditions are considered which make $\Gamma_o = -|\Gamma_o|$ at $z' = 0$; *i.e.*, for image terminated transmission conditions in the z direction. The integration yields

$$P_{yo} = \frac{k_y}{\omega\mu} |A_o|^2 h \left[(1 + |\Gamma_o|^2)w - 2|\Gamma_o| \frac{\sin k_{zo}w}{k_{zo}}\right].$$

The power in the dielectric section in the y direction crossing any given cross section is similarly

$$P_{y\epsilon} = \frac{k_y}{\omega\mu} |A_\epsilon|^2 h \left[(1 + |\Gamma_\epsilon|^2)d + 2|\Gamma_\epsilon| \frac{\sin k_{z\epsilon}d}{k_{z\epsilon}}\right].$$

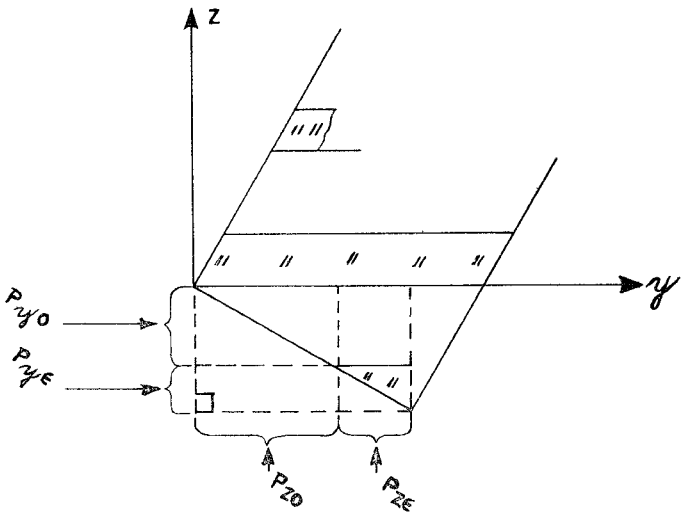

Fig. 5—Components of power flow across any given transverse cross section.

The total power is then the sum

$$P_T = P_{zo} + P_{z\epsilon} + P_{yo} + P_{y\epsilon}. \tag{21}$$

The continuity of the z components of the Poynting vector at the interface between the air section and dielectric section requires that

$$k_{zo}|A_o|^2[1 - |\Gamma_o|^2] = k_{z\epsilon}|A_\epsilon|^2[1 - |\Gamma_\epsilon|^2]. \tag{22}$$

A knowledge of the dimensions of the line and frequency then allows a determination of the magnitude of $|A_o|$ in terms of $|A_\epsilon|$. Quantitative values for the field quantities of (1) through (6) can then be obtained by expressing $|A_o|^2$ in terms of the total power transmitted by the line. The constant A_o for a given air section will lead in phase that of the next air section by angle Φ_I. This is true also for A_ϵ of dielectric sections.

Under the low frequency approximation previously considered, (32) reduces to

$$P_T \cong \left[|A_o|^2 \frac{4(1 - k_{eff}\sin^2\theta)}{[(1 - k_{eff}\sin^2\theta)^{1/2} + k_{eff}^{1/2}\cos\theta]^2}\right] \cdot \frac{kk_{eff}^{1/2}}{\omega\mu} h \frac{w + d}{\sin\theta} \tag{21a}$$

which agrees directly with that obtained directly from the fields using low frequency approximation; the bracketed term is $|E_{xo}|^2 \equiv |E_{x\epsilon}|^2$. In terms of the voltage, $V = |E_{xo}|h$, the total power is

$$P_T \cong \frac{V^2}{\dfrac{\omega\mu}{kk_{eff}^{1/2}} \dfrac{h}{(w + d)/\sin\theta}} = \frac{V^2}{Z_{opp}}$$

where Z_{opp} is recognized to be the characteristic impedance of the parallel plate line having a dielectric material with the dielectric constant k_{eff}.

Attenuation

The loss per unit length is the same at any given cross section and the same is true for the attenuation. For greater clarity, however, the loss per section will be calculated and the attenuation computed in this way.

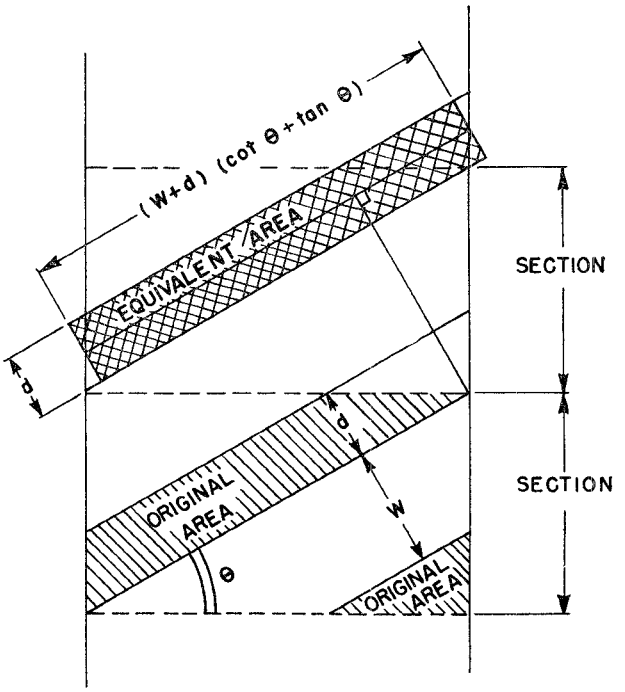

Fig. 6—Equivalent dissapative area under dielectric.

Conductor Losses

The component of field H_y gives rise to surface currents in the conductor planes in the z direction and the field H_z to currents in the y direction. Consider first the currents in the z direction for that portion of metal surface in contact with the dielectric. Shown in Fig. 6 is the original area per section in contact with one metal plane conductor and the equivalent area in terms of both the total original area and also the magnitude of the magnetic fields to which the surface is subjected.

The equivalent area can be seen to be built up of an equivalent piece taken from the original area and the substitution of equivalent areas above and below the field symmetry line. The power dissipated per section in the conductor walls under the dielectric by currents in the z direction is then, assuming negligible reaction on the modal character,

$$D_{\epsilon z} = 2(w + d)(\cot\theta + \tan\theta)R_s \int_{-d/2}^{+d/2} |H_y|^2 dz''$$

where R_s is the surface resistivity of the conductor.

Upon integration, this expression becomes

$$D_{\epsilon z} = 2\left(\frac{k_{z\epsilon}}{\omega\mu}\right)^2 |A_\epsilon|^2 R_s d(w + d)(\cot\theta + \tan\theta) \cdot\left[1 + |\Gamma_\epsilon|^2 - 2|\Gamma_\epsilon| \frac{\sin k_{z\epsilon}d}{k_{z\epsilon}d}\right].$$

A similar integration yields for the power dissipated per section by currents in the y direction,

$$D_{\epsilon y} = 2\left(\frac{k_y}{\omega\mu}\right)^2 |A_\epsilon|^2 R_s d(w + d)(\cot\theta + \tan\theta) \cdot\left[1 + |\Gamma_\epsilon|^2 + 2|\Gamma_\epsilon| \frac{\sin k_{z\epsilon}d}{k_{z\epsilon}d}\right].$$

By a similar determination of the equivalent area per section for the walls enclosing the air dielectric section, the power dissipated per section by currents in the z direction may be determined to be

$$D_{oz} = 2\left(\frac{k_{zo}}{\omega\mu}\right)^2 |A_o|^2 R_s w(w + d)(\cot\theta + \tan\theta) \cdot\left[1 + |\Gamma_o|^2 + 2|\Gamma_o| \frac{\sin k_{zo}w}{k_{zo}w}\right]$$

and the power dissipated per section in the y direction is

$$D_{oy} = 2\left(\frac{k_y}{\omega\mu}\right)^2 |A_o|^2 R_s w(w + d)(\cot\theta + \tan\theta) \cdot\left[1 + |\Gamma_o|^2 - 2|\Gamma_o| \frac{\sin k_{zo}w}{k_{zo}w}\right].$$

The total dissipation per section in the conductors is then

$$D_c = D_{\epsilon z} + D_{ey} + D_{oz} + D_{oy}. \tag{23}$$

The attenuation constant arising from attenuation in the walls is then

$$\alpha_c = \frac{1}{2}\frac{D_c}{P_T}\frac{\cos\theta}{w + d} \tag{24}$$

where P_T is given by (21) and the factor $\cos\theta/w+d$ converts the dissipation per section to that per unit length.

Again, the low frequency assumption reduces (23) such that when combined with (21) the expression for attenuation becomes identical to that calculated directly from the low frequency field equations, namely,

$$\alpha_{cLF} \cong \frac{R_s}{\left(\frac{\omega\mu}{kk_{eff}^{1/2}}\right)}\cdot\frac{1}{h} = \frac{R_s\frac{\sin\theta}{w + d}}{Z_{opp}}. \tag{24a}$$

Dielectric Losses

Power dissipated per section in dielectric is given by

$$D_\epsilon = (w + d)(\cot\theta + \tan\theta)h\omega\epsilon\tan\delta\int_{-d/2}^{d/2} |E_x|^2 dZ''$$

where $\tan\delta$ is the loss tangent of the dielectric and ϵ is the absolute dielectric constant. Upon integration, the dissipated power becomes

$$D_\epsilon = \omega\epsilon\tan\delta\,|A_\epsilon|^2 h(w + d)d(\cot\theta + \tan\theta) \cdot\left[1 + |\Gamma_\epsilon|^2 + 2\Gamma_\epsilon\frac{\sin k_{z\epsilon}d}{k_{z\epsilon}d}\right] \tag{25}$$

That portion of the attenuation resulting from dielectric losses is then

$$\alpha_\epsilon = \frac{1}{2}\frac{D_\epsilon}{P_T}\frac{\cos\theta}{W + d}. \tag{26}$$

The low frequency approximation for the attenuation resulting from dielectric losses is given by

$$\alpha_{\epsilon LF} = \frac{\omega\epsilon\tan\delta\frac{d}{w + d}}{2\left(\frac{kk_{eff}^{1/2}}{\omega\mu}\right)} = \frac{1}{2}\left(\frac{k_\epsilon}{k_{eff}^{1/2}}\right)\left(\frac{d}{w + d}\right)k\tan\delta. \tag{26a}$$

Application of Analysis to Coaxial Line with Helical Support

The phase constants, guide wavelength, and critical frequencies calculated for the equivalent parallel plate structure are assumed to be identical to those for the corresponding coaxial line, where, as initially indicated, the mean periphery of the coaxial line corresponds to the width of equivalent parallel plate. This same equivalence has been used to calculate the cutoff frequencies of coaxial line with good accuracy.[3]

To determine the attenuation of the coaxial line, the ratio of actual attenuation to that of the low frequency approximation is assumed to be the same for that of the coaxial line as for the equivalent parallel plate structure. Thus, for a coaxial line with helical dielectric support, attenuation resulting from conductor losses becomes

$$\alpha_{cc} = \frac{1}{2}\frac{\left(\frac{R_{si}}{\pi d} + \frac{R_{so}}{\pi D}\right)}{Z_o}\frac{\alpha_c}{\alpha_{cLF}} \tag{27}$$

[3] S. A. Schelkunoff, "Electromagnetic Waves," N. Y., D. Van Nostrand Co., Inc., 1951, p. 327, Fig. 8.51.

where Z_o is the characteristic impedance of the cable, R_{si} and d are respectively the surface resistivity and diameter of the inner conductor, R_{so} and D are respectively the surface resistivity and diameter of the outer conductor, α_{cLF} is the low frequency approximation for the parallel plate conductor attenuation obtained from (24a) and α_c is the actual value for the parallel plate conductor attenuation from (24). The attenuation resulting from dielectric losses is given by

$$\alpha_{\epsilon c} = \frac{k_\epsilon d}{w+d}\,\frac{Z_o}{Z_{oo}}\,\frac{\pi}{\lambda}\tan\delta\cdot\left(\frac{\alpha_\epsilon}{\alpha_{\epsilon LF}}\right) \tag{28}$$

where Z_o is the usual low frequency value of characteristic impedance of the cable, such as would be obtained from capacitance measurements, Z_{oo} is the characteristic impedance of the cable with dielectric removed, $\alpha_{\epsilon LF}$ is the low frequency approximation for the attenuation of the parallel plate which is due to dielectric losses as given in (26a) and α_ϵ is the actual attenuation of the parallel plate line caused by dielectric losses as given in (26). The total attenuation for the coaxial line is

$$\alpha_{Tc} = \alpha_{cc} + \alpha_{\epsilon c}. \tag{29}$$

The impedance of the cable and its possible variation with frequency requires further investigation.

Calculated Performance of ½ Inch 50 ohm Styroflex Line and Comparison with Measurements

Using the foregoing analysis, the propagation constants, some cutoff frequencies, and the attenuation in the dominant mode were calculated using the following dimensions for ½ inch Styroflex line:

Conductor	.165″
Helix-Width	.0985″
Helix-Lay	.564″
Helix-O.D.	.380″
Binder-Tape 3 Tapes	.907″ × .00473″
Binder-O.D.	.408″
Aluminum Sheath I.D.	.421″
Aluminum Sheath O.D.	.500″

The dimensions for the equivalent parallel plate line and other constant used were the following values:

$$h = \frac{.421 - .165}{2} = .128''$$

$$d = .0985''$$

$$\tan\theta = \frac{\pi(.421 + .165)}{2 \times .564} \quad (\theta = 32°)$$

$w = .564\cos\theta - .0985'' = .380''$
Polystyrene $k_\epsilon = 2.56$; $\tan\delta = .0002$
Surface Resistivity of Copper $= R_s = 2.61 \times 10^{-7}\sqrt{f}$
Surface Resistivity of Aluminum $= R_{sA} = 3.26 \times 10^{-7}\sqrt{f}$.

The effect of the binder tapes is neglected, the helix tape being assumed to extend to the outer conductor.

The critical frequencies calculated are tabulated as follows:

$n=0$	Condition	$n=1$	Condition
11.31 kmc/sec	(A)	20.44 kmc/sec	(C)
14.41 kmc/sec	(B)	23.56 kmc/sec	(D)
24.59 kmc/sec	(C)		

The chief band of interest is that between the frequencies zero and 11.31 kmc/sec. An attenuation band for propagation in the z direction exists between 11.31 and 14.41 kmc/sec with a second pass band appearing between 14.41 and 24.59 kmc/sec. The corresponding conditions of Table I are listed along with the frequencies. For $n=1$ in (17), and the conditions indicated in Table I, two other critical frequencies are calculated. An attenuation band exists between (C) and (D). From the above computations, there appears to be no higher mode interference in the chief band of interest.

TABLE II

Analysis of Operation
Dominant Mode

Frequency	$\frac{k_y}{k}$	$\frac{k_{zo}}{k}$	$\frac{k_{z\epsilon}}{k}$	$\left(\frac{\lambda}{\lambda_g}\right)$	Γ_o	Γ_ϵ	P_z	P_{yo}	$P_{y\epsilon}$	$\frac{f}{f_c}$
kmc/sec							%	%	%	
0	.610	.793	1.480	1.150	− .103	.206	71.9	22.3	5.8	0
6.28	.615	.789	1.478	1.160	− .154	.263	71.8	21.7	6.5	.55
8.24	.620	.784	1.476	1.169	− .219	.333	71.2	21.3	7.5	.729
9.90	.630	.777	1.472	1.189	− .363	.440	69.2	21.3	9.5	.875
10.48	.640	.768	1.468	1.207	− .480	.583	64.6	22.3	13.1	.927
11.03	.660	.751	1.459	1.244	− .698	.869	42.7	23.8	33.5	.975
11.31	.685	.728	1.447	1.292	−1.0	1.0	0	44.6	55.4	1.0

Shown in Table II above, for the parallel plate equivalent corresponding to ½ inch Styroflex, are values of phase constants divided by the free space phase constant; the square of the ratio of free space wavelength divided by the guide wavelength, $(\lambda/\lambda_g)^2$; the reflection coefficients associated with propagation in the z direction; and the percentages of power in given directions in air and dielectric all tabulated as a function of fre-

quency. As indicated in the relative frequency scale of the table, significant changes in the data are confined to the frequencies beyond $\frac{1}{2}$ the critical frequency for dominant mode operation. This is for the most part beyond the range at present considered for commerical use of the cable.

The over-all change in (k_y/k) is $+12.4$ per cent, that for (k_{zo}/k) is -8.2 per cent and that for $(k_{z\epsilon}/k)$ is -2.3 per cent. These changes in themselves are nominal and do not reflect the strong changes in the direction of power flow which takes place as the critical frequency is approached. The quantity, (λ/λ_y), shows that the guide wavelength decreases with frequency at a greater rate than the free space wavelength. For the low frequency approximation (λ/λ_g) is equivalent to the square root of the relative dielectric constant. Continuing this concept, it would be expected that there is a factor which reduces the characteristic impedance by the percentage change in the values of (λ/λ_g) over its zero frequency value. Further investigation is required before a useful value of impedance can be proposed since the influence of changes in field pattern has not as yet been considered.

The values of reflection coefficient Γ_o and Γ_ϵ are noted to have finite values at zero frequency. The electric field is uniform at low frequencies primarily because there is insufficient phase variation for the reflection coefficients to exert their effect. At the critical frequency, however, the variation acts like a complete standing wave in the z direction. This variation is depicted in Fig. 7 where the relative magnitude of electric field is

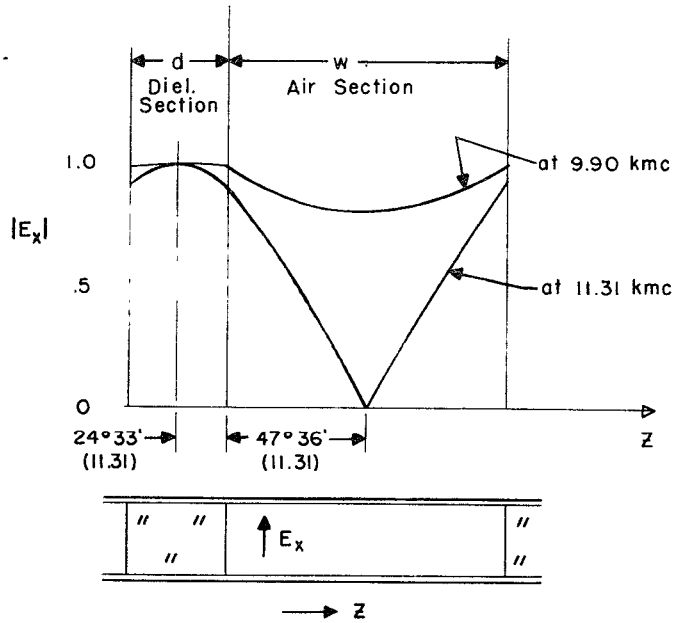

Fig. 7—Variation of electric field in cross section.

plotted as a function of distance in the z direction for 11.31 kmc/sec. This variation has a discontinuous derivative at the interface between air and dielectric as noted from the indicated angles. The variation would be of identical character in the transverse cross section of the line. In the coaxial line with helical support the corresponding cross sectional field pattern would have one zero and one maximum in the variation with angle. The distribution for lower frequencies lacks the zero value but has minimum and maximum fields at the same locations as illustrated in Fig. 7 by a plot of the relative field variation at 9.9 kmc/sec.

The power crossing any given cross section can be arbitrarily broken up into the power in the z direction, P_z; the power in the y direction in the air section, P_{yo}; and the power in the y direction in the dielectric section, $P_{y\epsilon}$; as indicated in Fig. 5. The proportioning for the low frequency approximation, indicated as zero frequency in Table II, could be arrived at using a TEM mode and simple geometry. The power in the z direction (perpendicular to the dielectric) is the largest proportion because the dielectric makes an angle of 32 degrees with the transverse direction. The total power in the y direction divides in proportion to the widths of the sections. The major change up to about 10.0 kmc/sec is the gain of power in the dielectric section, a familiar effect for microwave transmission lines. Further increase in frequency causes the propagation in the y direction to mount rapidly being entirely in the y direction at the critical frequency. At these higher frequencies, the efficiency could be expected to be seriously impaired because of the distorted mode and length of path of transmission.

Using the foregoing analysis, the attenuation values were calculated for $\frac{1}{2}$ inch Styroflex cable for all frequencies up to 11.31 kmc/sec, first critical frequency.

For the equivalent parallel plate line, the analysis gives exactly the ratio of the actual attenuation to the attenuation calculated using the low frequency approximation. Table III lists separately these ratios for

TABLE III

Attenuation Data for $\frac{1}{2}$ Inch O.D. Styroflex Cable

Freq. in kmc	Correction Factor Parallel Peak		Coax Line Low Freq. Approx.	
	$\frac{\alpha_c}{\alpha_{cLF}}$	$\frac{\alpha_\epsilon}{\alpha_{\epsilon LF}}$	α_{coLF}	$\frac{\alpha_{\epsilon LF}}{\tan\delta=.0003}$
0	1	1	0	0
2	1.003	1.011	3.517	.7632
4	1.008	1.035	4.974	1.526
6.28	1.028	1.112	6.23	2.396
8.24	1.06	1.31	7.14	3.144
9.9	1.232	1.576	7.829	3.778
10.48	1.413	2.153	8.05	3.999
11.03	1.915	5.329	8.259	4.209
11.31	4.069	6.849	8.364	4.316

the attenuation caused by conductor loss and that caused by dielectric loss. These factors are assumed to apply as correction factors to the attenuation of the coaxial structure calculated by the use of the low frequency approximation. These coaxial attenuation values are also listed in Table III for a dielectric loss

tangent of 0.0003. The curves for the corrected values of coaxial attenuation are shown plotted separately in Fig. 8 for the conductor and dielectric loss. The attenuation caused by conductor loss is noted to predominate virtually over the entire frequency band in spite of the fact that there is a more marked correction factor for the attenuation caused by dielectric loss.

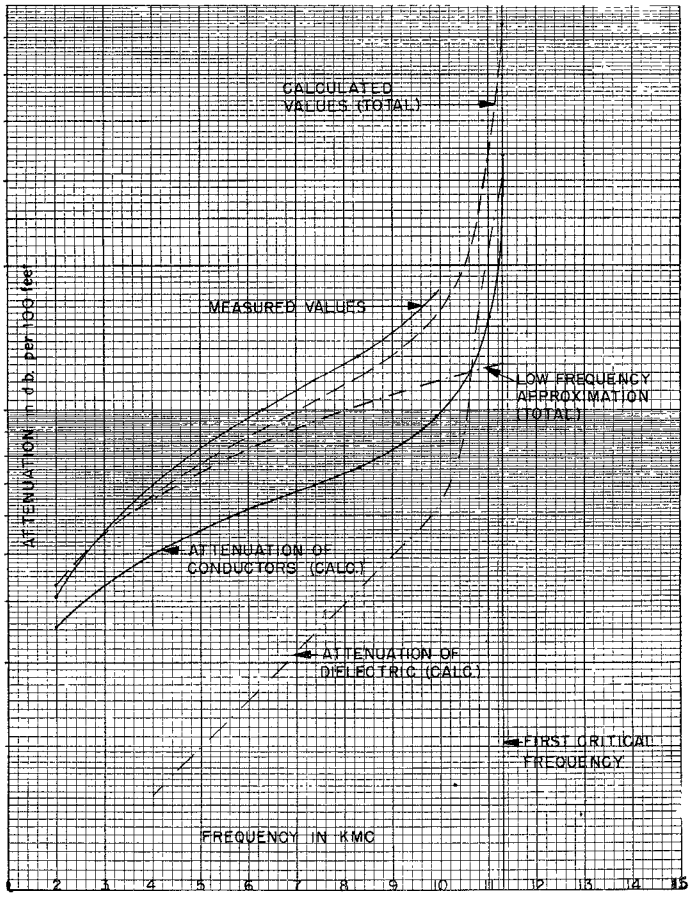

Fig. 8—Attenuation vs frequency, ½ inch O.D. 50 ohm Styroflex cable. Loss Tangent = 0.0003.

The total calculated attenuation is plotted in Fig. 8 along with curves for measured values[4] and the total attenuation obtained from the use of the low frequency approximation. In particular, the attenuation values for the low frequency attenuation do not contain the rise toward peak values as the critrical frequency is approached, whereas the measured values and the values calculated from the foregoing analysis do show this rise; use of the logarithmic scale for attenuation should be noted. From the curve it is evident that the application of the correction factors of Table III appears to be warranted for frequencies above 4.0 kmc/sec. At 9.9 kmc/sec, the attenuation value for the low frequency approximation is 30 per cent below that of the more complete analysis. The agreement between measured values and those of the analysis are dependent on the value used for the loss tangent of the dielectric. A loss tangent value of 0.0003 which is representative of polystyrene at these frequencies was chosen for the calculated curve of attenuation for Fig. 8. At 9.9 kmc/sec, the measured value is 7.4 per cent above the calculated value. In view of the overlap of calculated and measured values at 2.5 kmc/sec, a lower value of loss tangent is perhaps appropriate for the lower frequencies. The measured values can be expected to exceed the calculated values because the measured surface resistance values of the metal are known to exceed theoretical values, particularly for frequencies approaching 10.0 kmc/sec. This effect would be emphasized by the existence of transverse components of surface currents which the analysis indicates. Further detailed investigation would be necessary to warrant closer detailed examination of the agreement between the theoretical and experimental results.

[4] Measured at Signal Corps Engineering Laboratories.

Comments

An equivalent parallel plate structure has been used to analyze the frequency limitations and performance characteristics of a coaxial line with a helical dielectric support. The key to equivalence of the parallel plate and coaxial structure is the imposed boundary condition that, at any given transverse cross section for the parallel plate, the fields at the sides are identical in magnitude and phase angle. An analysis in terms of component transmission lines, one parallel to the dielectric and the other perpendicular to the dielectric, may then be used to determine the detailed fields and their variation with frequency. The performance of the overall transmission line reflects the iterative line characteristics of the component transmission line perpendicular to the dielectric, and gives rise to pass bands and high attenuation bands for the over-all transmission line.

For ½ inch Styroflex transmission line, analysis based on the low frequency approximation, which assumes cross sectional fields independent of angle and an equivalent dielectric constant corresponding to the air and dielectric sections in parallel, is accurate up to about 4.0 kmc/sec or about 35 per cent of the cutoff frequency. Above this frequency, the analysis indicates that the power component in the dielectric directed parallel to the dielectric grows at the expense of the power component directed perpendicular to the helix while the power component in the air directed parallel to the helix remains, for the most part, reasonably constant. The increase of the field in the dielectric corresponds with a reduction in the guide wavelength and would imply a reduction in the characteristic impedance of the line. Similar behavior would be expected for other coaxial lines with a helical dielectric support, but the details of operation would be dependent on the proportion of dielectric and the pitch angle.

In the analysis, the line has been assumed smooth in the direction parallel to the helix. Precise construction of the line would be necessary to maintain this condition since it is evident that eccentricity would give rise to a line with periodicities in this direction.